ANTIMICROBIAL AGENTS AND CHEMOTHERAPY, Nov. 2005, p. 4689–4699 Vol. 49, No. 11
0066-4804/05/$08.00+0 doi:10.1128/AAC.49.11.4689–4699.2005

Mouse Adenovirus Type 1 Infection in SCID Mice: an Experimental Model for Antiviral Therapy of Systemic Adenovirus Infections

L. Lenaerts,[1] E. Verbeken,[2] E. De Clercq,[1] and L. Naesens[1]*

Rega Institute for Medical Research, Division of Virology and Chemotherapy,[1] and Division of Morphology and Molecular Pathology,[2] Katholieke Universiteit Leuven, B-3000 Leuven, Belgium

Received 3 June 2005/Returned for modification 15 July 2005/Accepted 16 August 2005

The importance of human adenovirus infections in immunocompromised patients urges for new and adequate antiadenovirus compounds. Since human adenoviruses are species specific, animal models for systemic adenovirus infections rely on a nonhuman adenovirus. We established mouse adenovirus type 1 (MAV-1) infection of BALB/c SCID mice as a model for the evaluation of antiadenovirus therapy. In vitro studies with mouse embryonic fibroblasts pointed to the acyclic nucleoside phosphonate cidofovir and the N-7-substituted acyclic derivative 2-amino-7-(1,3-dihydroxy-2-propoxymethyl)purine (S-2242) as markedly active compounds against MAV-1. SCID mice, infected intranasally with MAV-1, developed a fatal disseminated infection after approximately 19 days, characterized by hemorrhagic enteritis. Several techniques were optimized to monitor viral, immunological, and pathological aspects of MAV-1 infection. Real-time PCR quantification of viral DNA revealed that after replication in the lungs, virus disseminated to several organs, including the brain, liver, spleen, intestine, heart, and kidneys (resulting in viruria). Immunohistochemical staining showed that MAV-1 was localized in the endothelial cells of the affected organs. Using reverse transcription-PCR, tissue levels of proinflammatory cytokines (i.e., interleukin-1β and tumor necrosis factor alpha) were found to be markedly increased. The MAV-1/SCID model appears to be an appropriate model for in vivo evaluation of antiadenovirus agents. Treatment with cidofovir or S-2242 at a dose of 100 mg per kg of body weight resulted in a significant delay in MAV-1-related death, although these antivirals were unable to completely suppress virus replication despite continued drug treatment. These findings suggest that complete virus clearance during antiviral therapy for disseminated adenovirus infection may require an efficient adaptive immune response from the host.

Adenoviruses are ubiquitous agents that are associated with diverse clinical syndromes, ranging from respiratory infections, conjunctivitis, gastroenteritis, hepatitis, and hemorrhagic cystitis to neurological disorders. While adenovirus infections in the immunocompetent host are mostly mild and self-limiting, they result in high morbidity and mortality in immunocompromised patients. For instance, in pediatric patients undergoing allogeneic stem cell transplantation, mortality rates as high as 60% have been reported for disseminated adenovirus infection (56). During the last two decades, severe adenovirus infections have increased in frequency due to the growing number of transplantation patients and the emergence of the human immunodeficiency virus epidemic (27). At present, there is no formally approved antiviral therapy for adenovirus infections. Among currently available antiviral agents, only a few have shown promise in treating adenovirus disease. Treatment with the nucleoside analogue ribavirin has yielded conflicting results and seems to be ineffective in patients who are at high risk for disseminated adenovirus disease (5, 15, 30). The nucleotide analogue cidofovir, with potent in vitro activity against herpesviruses, polyomaviruses, and different serotypes of adenoviruses, has been shown to be a therapeutic option for life-threatening adenovirus diseases (5, 19, 21, 31). The dose-limiting toxicity of cidofovir is nephrotoxicity, but this can be diminished by coadministration of probenecid, an infrequent treatment schedule, and sufficient hydration (29). There is an increasing need for new antiadenovirus drugs with improved activity and safety profiles to direct therapy for life-threatening or debilitating adenovirus infections.

Since adenoviruses are species specific, an understanding of the mechanism by which adenoviruses cause disease depends on the development of a relevant animal model. Currently, no satisfactory model exists for the evaluation of antiviral therapy against disseminated adenovirus disease. In mice and cotton rats, intranasal infection with human adenovirus type 5 produces inflammatory pneumonia, although virus replication is restricted to the synthesis of early adenovirus proteins (16, 45). On the other hand, human adenovirus type 5 is able to replicate in the eyes of cotton rats and New Zealand rabbits, causing localized but no disseminated disease (17, 25, 55). Models with mouse adenovirus type 1 (MAV-1) permit the study of a replicating adenovirus in vivo. Inoculation of mice with MAV-1 results in a systemic infection of cells of the mononuclear phagocyte system and microvascular endothelial cells (10, 24). MAV-1 can cause fatal disease in newborn and adult mice, but the outcome of the infection depends on the virus dose, immune status, and mouse strain. Adult mice with a C57BL/6 background succumb to hemorrhagic encephalitis following infection with MAV-1 (10, 18, 28, 52), whereas mice with a BALB/c background are resistant (10, 18). Immunodeficient BALB/c mice are highly susceptible to MAV-1 infection and die from a nonneurological disease with prominent involve-

* Corresponding author. Mailing address: Rega Institute for Medical Research, K. U. Leuven, Minderbroedersstraat 10, B-3000 Leuven, Belgium. Phone: 32-16-337345. Fax: 32-16-337340. E-mail: lieve.naesens@rega.kuleuven.ac.be.

ment of the liver and intestinal tract (10, 38, 43). A few studies have been published describing MAV-1 infection of severe combined immunodeficient (SCID) mice with a BALB/c background. Charles and colleagues reported a generalized and fatal nonneurologic infection of MAV-1 in BALB/c SCID mice with focal hemorrhagic enteritis (10). In the CB-17 SCID model of Pirofski et al., MAV-1 induces microvesicular fatty hepatocyte degeneration similar to that observed in human Reye syndrome (43).

Based on these findings, we established MAV-1 infection of BALB/c SCID mice in which the virus causes a fatal disseminated disease characterized by hemorrhagic enteritis. Following a profound study of the pathological, inflammatory, and viral aspects of the infection, we used this unique experimental model for the evaluation of antiviral agents for the treatment of systemic adenovirus infections representative of life-threatening and debilitating adenovirus dissemination in immunocompromised patients.

MATERIALS AND METHODS

Cells and viruses. The C3H/3T3 mouse embryonic fibroblast cell line, originally established by Billiau et al. (4), was subcultivated in Dulbecco's minimal essential medium supplemented with 0.075% bicarbonate, 1 mM sodium pyruvate, and 10% heat-inactivated newborn calf serum, which was reduced to a concentration of 2% for the antiviral studies.

Mouse adenovirus type 1 strain FL (MAV-1) was obtained from the American Type Culture Collection. Virus stocks were prepared in C3H/3T3 cells. When ~90% cytopathic effect was reached (at day 10 to 12 postinfection [p.i.]), culture flasks were frozen at −80°C. After cell lysis by rapid thawing and centrifugation at 1,800 × *g*, the clarified culture supernatant was divided into aliquots and stored at −80°C to be used in the antiviral in vitro experiments. The titer of the virus stock was determined using a standard plaque assay (54) and yielded a titer of $\sim 10^6$ PFU per ml. For in vivo experiments, MAV-1 particles were purified from the clarified culture supernatant by chromatographic purification using the Virapur kit (Virapur LLC, San Diego, CA) according to the manufacturer's instructions. The titer of this virus stock was $\sim 10^4$ PFU per ml, corresponding to $\sim 10^{10}$ viral particles per ml, as determined by real-time PCR analysis. C3H/3T3 cells and virus stocks were free of *Mycoplasma* contamination by PCR analysis.

Chemical compounds. The structures and origins of the test compounds were as follows: cidofovir [(*S*)-1-(3-hydroxy-2-phosphonylmethoxypropyl)cytosine {(*S*)-HPMPC; Vistide}] was from Gilead Sciences, Foster City, CA; (*S*)-HPMPA [(*S*)-9-(3-hydroxy-2-phosphonylmethoxypropyl)adenine] and HPMPO-DAPy {2,4-diamino-6-[3-hydroxy-2-(phosphonomethoxy)propoxy]pyrimidine} were from A. Holý, Prague, Czech Republic; acyclovir (Zovirax), ganciclovir (Cymevene), zalcitabine (ddC; Hivid), and ribavirin (Virazole) were from commercial sources; S-2242 [2-amino-7-(1,3-dihydroxy-2-propoxymethyl)purine] was from I. Winkler, Hoechst Inc., Frankfurt am Main, Germany; alovudine (3′-fluoro-3′-deoxythymidine; FddT) was from P. Herdewijn, Leuven, Belgium; and A-5021 {(1′*S*,2′*R*)-9-[[1′,2′-bis(hydroxymethyl)-cycloprop-1′-yl]methyl]guanine} was from Ajinomoto, Inc., Kawasaki, Japan.

Antiviral in vitro experiments. C3H/3T3 cells were seeded in 96-well plates at 17,000 cells per well and incubated for 4 days until confluence was reached. To each well, 50 μl of MAV-1 was added, diluted in medium to obtain a multiplicity of infection of ~0.01 PFU per cell. After 2 h at 37°C, virus was aspirated and replaced by serial dilutions of the test compounds (200 μl per well). Mock-treated cultures receiving only the test compounds were included in each plate. After 8 to 10 days of incubation at 37°C, microscopy was performed to score the virus-induced cytopathic effect (CPE). The plates were then subjected to the MTS-based colorimetric assay for cell viability according to the manufacturer's instructions (Promega, Leiden, The Netherlands). The A_{490} values, corrected for cytotoxicity exerted by the test compounds (as determined in mock-infected cultures), were used to calculate the percent cell viability. The 50% effective concentration (EC_{50}) was determined by extrapolation and defined as the compound concentration that produced 50% protection against the virus.

In a separate set of plates, C3H/3T3 cells were infected and treated with the compounds as described above and used to measure virus replication at 8 to 10 days after MAV-1 infection. After removal of the culture supernatant, cells and virus particles were lysed by the addition of 70 μl of lysis buffer (10 mM Tris · HCl, pH 7.8, 0.5% sodium dodecyl sulfate, 5 mM Na_2EDTA, and 80 μg/ml proteinase K) and incubated for 1 h at 50°C, followed by 20 min at 65°C for proteinase K inactivation. After clarification (23,000 × *g*, 10 min), cell extracts were stored at −20°C until real-time PCR was performed as described below. The EC_{50} was calculated by extrapolation as the compound concentration at which the number of viral particles at 8 to 10 days p.i. was 50% compared to the value obtained for the virus control.

The cytostatic activity of the test compounds was determined in proliferating C3H/3T3 cells seeded at 15,000 cells per well in 96-well trays and treated with serial compound dilutions for 3 days, after which the cells were counted in a Coulter Counter. The CC_{50} was defined as the compound concentration that produced 50% inhibition of cell proliferation.

Antiviral in vivo studies. Five- to seven-week-old C.B-17/Icr scid/scid (FOX CHASE SCID) mice weighing 16 to 20 g were used in all experiments. The animals were bred at the Rega Institute under specific-pathogen-free conditions. Males and females were equally distributed over the different treatment conditions (10 mice per treatment condition). Mice were given light ether anesthesia and intranasally infected with 300 PFU in a volume of 20 μl of phosphate-buffered saline (PBS). Antiviral therapy with cidofovir or S-2242 was started 4 h prior to infection. The compounds were administered subcutaneously at 100 mg per kg of body weight. Treatment with cidofovir was continued for 5 consecutive days p.i. and then on alternate days; S-2242 treatment was given by daily injection. Placebo mice were treated subcutaneously with PBS on alternate days. Drug administration was continued until the death of the animals. To assess drug-associated toxicity, uninfected animals were administered cidofovir or S-2242 according to the same scheme as described for the virus-infected animals. To monitor toxicity, the body weight of all mice was recorded daily. All animal studies were conducted according to the guidelines of the Ethical Committee of our university. For statistical analyses, *P* values were calculated with a two-tailed Student's *t* test.

Histopathology and immunohistochemistry. At predetermined time points, mice were killed and subjected to extensive transcardial perfusion with PBS. From the following organs, a part was fixated in 4% formaldehyde for 24 h and then embedded in paraffin: spleen, kidney, liver, small intestine, lung, heart, and brain. Tissue sections, 4 μm thick, were stained with hematoxylin and eosin for routine histologic examination and immunohistochemically stained with a rabbit polyclonal antibody to the MAV-1 E3 class 1 protein using a standard avidin-biotin immunoperoxidase staining procedure. The anti-E3 polyclonal antibody was prepared by immunizing rabbits with an antigenic peptide containing an amino acid sequence specific for the MAV-1 early protein E3 class 1, coupled to the immunogenic carrier protein KLH (KLH-KNA VRT GAG PDD ECF, synthesized by Eurogentec, Seraing, Belgium). On day 0, preimmunization serum was taken and the first immunization was done with 620 μg of the peptide-protein conjugate diluted in 1 ml complete Freund's adjuvant. Two boosters were given with 620 μg peptide-protein conjugate in 1 ml incomplete Freund's adjuvant on day 16 and day 37, respectively. Nineteen days later, rabbits were bled, and after affinity purification of the immunoglobulin G fraction in the serum (MAbTrap kit; Amersham Biosciences, Germany), optimal conditions for immunohistochemical staining were determined on liver and spleen tissue sections from MAV-1-infected mice.

Quantification of viral DNA. For the in vitro antiviral experiments, cell extracts, prepared as described above, were diluted 100-fold in water, after which 2 μl was added to optical plates containing 23 μl of qPCR MasterMix for SYBR green I (Eurogentec) and the forward and reverse primers at 300 μM. Primers, derived from GenBank sequences, were chosen to amplify a 167-bp fragment within the MAV-1 hexon DNA sequence (forward, 5′-GGCCAACACTACCG ACACTT-3′; reverse, 5′-TTTTGTCCTGTGGCATTTGA-3′). Real-time PCR analysis was performed in an ABI Prism 7000 apparatus (Applied Biosystems) and consisted of 10 min of initial denaturation at 95°C, followed by 40 thermal cycles of 15 s at 95°C and 90 s at 60°C. A dissociation profile was taken at the end of each analysis to confirm the specificity of the PCR amplification. In each individual experiment, a standard curve ($R^2 > 0.98$, within the range of 10^3 to 10^8 copies per reaction mixture) was obtained by amplification of known amounts of a pGEM-T vector in which a 743-bp fragment of MAV-1 hexon DNA was inserted using common cloning procedures. These standard curves were used to convert the cycle threshold values for the extracts into the absolute number of MAV-1 hexon DNA copies.

For the in vivo studies, quantification of viral DNA was performed as follows. Blood was collected from ether-anesthetized mice by heart puncture and treated with 20 μl 0.5 M Na_2EDTA. A 100-μl aliquot was used for DNA extraction using the QIAamp DNA blood mini kit (QIAGEN, Hilden, Germany). After perfusion with PBS and dissection, parts of the organs were homogenized and DNA was extracted following the instructions of the tissue protocol of the QIAamp DNA

TABLE 1. Activity against mouse adenovirus type 1 and human adenovirus type 2[a]

Compound	MAV-1-infected C3H/3T3 cells			Ad2-infected HEL cells[c]	
	EC_{50} (μM)		CC_{50} (μM)	EC_{50} (CPE assay) (μM)	CC_{50} (μM)
	CPE assay	MTS assay			
Acyclic nucleoside phosphonates					
Cidofovir	2.0 ± 0.3	2.2 ± 0.8	154 ± 20	2.0 ± 0.6	83 ± 25
(*S*)-HPMPA	1.4 ± 0.1	0.7 ± 0.4	134 ± 31	0.7 ± 0.3	12 ± 8
HPMPO-DAPy	0.8 ± 0.3	0.9 ± 0.3	>250	5.4 ± 1.7	54 ± 34
Acyclic nucleoside analogues					
Acyclovir	>1,000	>1,000	≥1,000	>1,000	>750
Ganciclovir	35 ± 7	14 ± 5	>1,000	39 ± 15	115 ± 14
S-2242	6.1 ± 2.5	3.7 ± 1.4	>250	0.6 ± 0.3	>400
2′,3′-Dideoxynucleoside analogues					
ddC	39 ± 11	39 ± 5	>250	1.4 ± 0.4	231 ± 184
FddT	1.9 ± 0.4	1.9 ± 0.4	>250	0.80 ± 0.48	ND[b]
Nucleoside analogue (ribavirin)	>1,000	>1,000	189 ± 80	>250	30 ± 18

[a] Values are means ± standard deviations of the results from three independent experiments.
[b] ND, not determined.
[c] Antiviral data for Ad2, as determined with human embryonic lung (HEL) fibroblasts, were taken from reference 39.

mini kit (QIAGEN). DNA extracts were diluted with water to a final concentration of 0.3 μg per μl prior to real-time PCR analysis. To ensure that the DNA extracts of infected organs did not possess PCR-inhibiting compounds, a twofold dilution series was subjected to real-time PCR analysis. Since there was no evidence for PCR inhibition, 2 μl of the DNA (≤0.3 μg per μl) was added to optical plates containing 23 μl of a mixture of qPCR MasterMix (Eurogentec), forward and reverse primers (900 nM final concentration), and *Taq*man probe (6-FAM–5′-CATTCCAGCCAACTTATGGCTCGGC-3′–BHQ-1, 200 nM final concentration). The forward and reverse primers were the same as described for real-time PCR analysis of cell extracts. To take into account experimental variations, the primer-probe set of the 18S genomic endogenous control kit (18S primer mix, 75 nM final concentration; 18S Yakima Yellow Dark-quenched probe, 100 nM final concentration; Eurogentec) was included in the same PCR mixture as the target primer-probe set. The thermal profile of the real-time PCR analysis was identical to that carried out in the in vitro experiments. In each individual experiment, two standard curves were included. The first was obtained by amplification of known amounts of the pGEM-T MAV-1 hexon vector construct, as described above. For the second, a series of known amounts of human male chromosomal DNA (18S genomic control kit; Eurogentec) was used to obtain a standard curve ($R^2 > 0.98$, within the range of 0.94 to 60 ng human male chromosomal DNA per reaction mixture) of the amplified 18S rRNA gene. These standard curves were used to convert the respective cycle threshold values for the extracts into the number of MAV-1 DNA copies per ng chromosomal DNA. The lower limit of detection was 14 MAV-1 DNA copies per ng chromosomal DNA.

Urine was collected from MAV-1-infected mice on alternating days and pooled from mice receiving the same treatment, and DNA was extracted using the QIAamp viral RNA mini kit (QIAGEN). Quantification of viral DNA was performed with real-time PCR as described for blood and tissue DNA extracts. A standard curve of known amounts of MAV-1 hexon DNA copies was prepared in a DNA extract prepared from the urine of uninfected mice. For each urine sample, the creatinine level was determined, and the amount of viral DNA in the urine samples was expressed as the logarithm of the number of MAV-1 DNA copies per microgram of creatinine.

Determination of cytokine mRNA levels in blood and dissected organs. Approximately 500 μl of total blood (collected from anesthetized mice by heart puncture and treated with 20 μl 0.5 M Na_2EDTA) was used for RNA extraction of leukocytes using the QIAamp RNA blood mini kit (QIAGEN). After dissection, parts of the organs were homogenized and RNA was extracted by following the instructions of the RNeasy mini kit (QIAGEN). Twenty-five microliters of the RNA extract was treated with 75 U RNase-free DNase (Roche, Basel, Switzerland) at 37°C for 45 min, followed by 10 min of incubation at 70°C to inactivate residual DNase activity. The absence of contaminating DNA was certified by a standard PCR detecting glyceraldehyde-3-phosphate dehydrogenase (GAPDH) DNA using 0.5 U Super*Taq* DNA polymerase (HT Biotechnologies, Cambridge, United Kingdom), 500 μM deoxynucleoside triphosphates, and 0.5 μM concentrations of the following primers: 5′-TCAACACCCCAGCC ATGTA-3′ and 5′-CAGGTCCAGACGCAGGAT-3′. PCR was performed as follows: 2 min of initial denaturation at 95°C; 40 thermal cycles of 30 s at 95°C, 45 s of annealing at 58°C, and 1 min of elongation at 72°C; and an additional final extension at 72°C for 5 min. Synthesis from 5 μl DNase-treated RNA was carried out using 0.5 μg of oligo$(dT)_{15}$ primers (Promega), 0.5 mM of each deoxynucleoside triphosphate (Invitrogen Life Technologies, Merelbeke, Belgium), 40 U porcine RNase inhibitor (Amersham Biosciences), and 200 U Moloney murine leukemia virus reverse transcriptase (Invitrogen Life Technologies) in a final reaction volume of 20 μl. For the mouse cytokines interleukin-6 (IL-6), gamma interferon (IFN-γ), IL-1β, and tumor necrosis factor alpha (TNF-α), PCR amplification was performed with the Multiplex cDNA kit (Biosource International, Camarillo, CA), while the detection of mouse chemokines MIG (monokine induced by interferon gamma), ENA-78, eotaxin, macrophage inflammatory protein 1 alpha (MIP-1α), and MIP-1β was performed with the MPCR kit for mouse chemokine genes set 2 (Maxim Biotech, Inc., San Francisco, CA). All PCR products were size separated on a 2% agarose gel and visualized under UV illumination after ethidium bromide staining. Quantification of expression levels was performed with Image Master 1D Elite software (Amersham Biosciences).

RESULTS

In vitro evaluation of antiviral compounds against MAV-1 in C3H/3T3 cells. For several classes of nucleoside and nucleotide analogues, the in vitro activity against MAV-1 was determined and compared with their respective activities against human adenovirus type 2 (Ad2). When 90 to 100% CPE was reached, the anti-MAV-1 activity was measured by two different methods, namely evaluation of the adenoviral cytopathic effect and cell viability determination by the formazan-based MTS assay. A close correlation was observed between the EC_{50}s obtained by the CPE and MTS assay (Table 1). The EC_{50}s obtained for the acyclic nucleoside phosphonates cidofovir and (*S*)-HPMPA were comparable to the values reported for Ad2 (39). The new derivative HPMPO-DAPy was found to be 2.5-fold more active than cidofovir against MAV-1 yet 2-fold less active than cidofovir against Ad2. This suggests that the activation of HPMPO-DAPy may be species dependent, although this should be further confirmed in biochemical studies. Among the acyclic nucleoside analogues evaluated, ganciclovir was found to be moderately active against MAV-1, in agreement with its modest activity against Ad2. The N-7-substituted acyclic nucleoside analogue S-2242, previously reported to be active against all human herpesviruses and pox-

viruses (41, 49), also proved active against MAV-1. Its activity against a wide range of DNA viruses can be explained by its independence from activation by virus-encoded kinases. No significant inhibition of MAV-1 replication was observed for acyclovir or ribavirin. The 2′,3′-dideoxynucleoside analogue FddT showed EC_{50}s and CC_{50}s for MAV-1 comparable to those for cidofovir. Although the 2′,3′-dideoxynucleoside analogue ddC displays potent and selective activity against human adenoviruses, it was much less active against MAV-1. This is likely due to the poor conversion of ddC to its 5′-triphosphate in murine cells (2). For the acyclic nucleoside phosphonate cidofovir and the acyclic nucleoside analogue S-2242, an additional evaluation of the anti-MAV-1 activity was performed by real-time PCR quantification of viral DNA as a direct parameter for virus replication. Extraction of total DNA from infected cells was performed as described by Naesens et al. (39). Real-time PCR analysis confirmed the data obtained by the CPE and MTS assay (data not shown). Overall, the correlation in the activities of these nucleoside and nucleotide analogues between human adenoviruses and MAV-1 is not quite unexpected, since the DNA polymerases of human adenoviruses and MAV-1 share about 57% amino acid similarity (35).

Establishment of the MAV-1/SCID model. C.B-17 SCID mice which carry the scid mutation and have a BALB/c genotype (except for the single locus of the C57BL/6Ka mice) were inoculated intranasally with MAV-1. A small titration study with 20, 100, and 500 PFU showed that, even at 20 PFU, MAV-1 caused 100% mortality, with the mean day of death being dose dependent and highly reproducible (data not shown). All subsequent studies were performed with a virus inoculum of 300 PFU. The first signs of disease became visible about 17 days p.i. and resulted in the abrupt onset of lethargy, ruffled fur, poor feeding, hunched posture, unsteady, mechanical gait, and hyperpnea. Death followed the onset of clinical illness within 24 h (Fig. 1). At day 7 and day 14 p.i. and at the time of severe sickness, 2 mice from each group were sacrificed. Gross pathological examination revealed no evidence of disease until the onset of clinical illness and showed that all moribund mice were succumbing to focal hemorrhagic enteritis, although the extent of inflammation showed some variation.

Histopathological and immunohistochemical analysis following MAV-1 infection. Upon histopathological evaluation of dissected organs, the sharp onset of MAV-1 pathology was confirmed. During the first 14 days p.i., there was neither pathology nor inflammation in any of the examined organs. At the time of severe illness of the infected mice, part of the small intestine showed acute necrotizing enteritis, characterized by mucosal and at times transmural necrosis of the intestinal wall, associated with a purulent neutrophilic infiltrate. In some cases, a few inflammatory foci of neutrophils or so-called microabscesses were encountered in liver, but all other organs examined appeared normal (Fig. 2). Since all in vivo studies were performed with purified MAV-1 particles, pathology induced by impurities in crude virus stocks (such as proinflammatory cytokines) could be excluded, and hence, the observed pathology solely resulted from viral replication (53). Using immunohistochemical staining with a polyclonal antibody directed toward MAV-1 E3, virus was not visible at 7 and 14 days p.i. but was clearly present at the time the infected mice were moribund. Viral antigen was most abundant in the intestine, liver, adrenal, and spleen tissues (Fig. 2). All examined organs stained positive for MAV-1 E3, except the kidneys, which showed weak or no positivity. In all organs, immunoreactivity was restricted to the endothelial cells, although in the liver, the presence of viral antigen was also demonstrated in parenchyma cells.

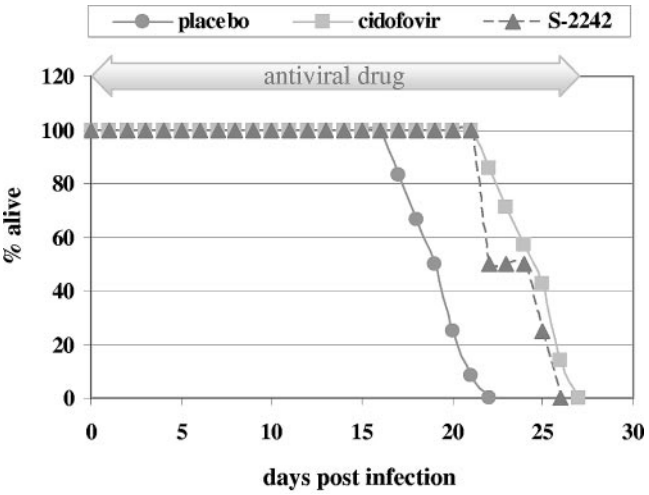

FIG. 1. Mortality curve of SCID mice intranasally infected with MAV-1 and treated with placebo, cidofovir (100 mg per kg), or S-2242 (100 mg per kg) (see Materials and Methods for dosing schedule). Data for the placebo- and cidofovir-treated mice are the means from two independent experiments, each including 10 mice per group. Values for the S-2242-treated mice are from one experiment including 10 mice.

To allow for a more detailed immunohistochemical monitoring of MAV-1 replication in infected organs, we also prepared a rabbit polyclonal antibody directed toward the MAV-1 hexon protein, a structural protein that is synthesized late in the replication cycle. Although the antihexon antibody gave satisfying results in Western blot analysis on MAV-1-infected fibroblast cells, it reacted aspecifically in Western blotting and immunohistochemical staining of MAV-1-infected tissues, making it unsuitable for our in vivo studies.

Quantification of viral loads in mice. To determine viral loads in the infected organs, real-time PCR analysis was performed on blood samples and perfused and homogenized parts of liver, lung, brain, heart, kidney, spleen, and intestine tissues. We measured viral DNA as a surrogate marker, since the real-time PCR method represents a reproducible, sensitive, and fast approach for estimation of viral load in a significant number of samples. As shown in Fig. 3a, at 7 days p.i., viral DNA was detected in liver, heart, kidney, spleen, and intestine tissues, with the highest concentration in the lungs of infected mice. At later time points, the viral DNA content of all tested organs gradually increased to reach a maximum in the succumbing placebo mice at day 20 p.i. As a noninvasive method to monitor viral replication, a real-time PCR assay was set up for the quantification of viral DNA in daily urine samples (Fig. 4). No viral DNA was detected in the urine of infected mice until day 15 p.i. Then the viral DNA concentration in urine showed a rapid increase, corresponding to the onset of clinical

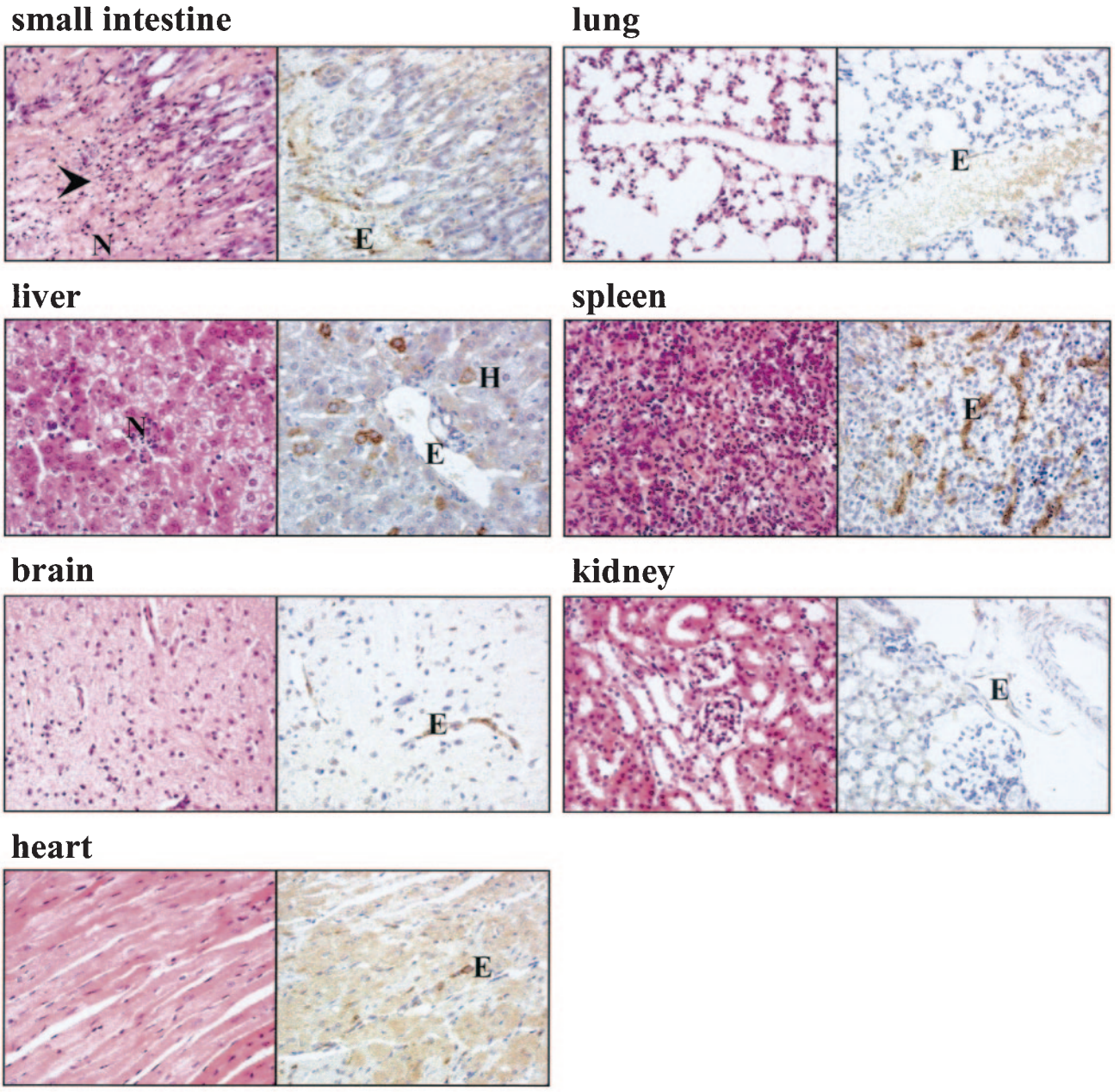

FIG. 2. Hematoxylin and eosin (left side) and immunohistochemical (right side) staining for MAV-1 E3 protein on representative sections of small intestine, liver, brain, heart, lung, spleen, and kidney tissues of a moribund placebo mouse (19 days p.i.). Infected cells show dark brown cytoplasmic staining for MAV-1 E3. Magnification, ×400. The arrowhead indicates a site of necrosis. E, endothelial cell; H, hepatocyte; N, neutrophils.

symptoms and coinciding with the virus titer increase in the organs, and further increased until the death of the infected mice. It was noteworthy that, despite the high levels of viral DNA in the urine and kidney extracts of MAV-1-infected mice, immunohistochemical staining of viral antigen in the kidneys of these mice was weak. A possible explanation may be that immunostaining is a less sensitive technique than real-time PCR, and hence, viral antigen may not be revealed by immunostaining if expressed at low levels.

Immunological aspects of MAV-1 pathology. Histopathological analysis of infected organs demonstrated the presence of inflammatory cells within the small intestine and liver of infected mice, suggesting that the host immune response may contribute to the MAV-1 pathology. To determine the type and extent of inflammatory response to MAV-1 infection, we measured the mRNA levels for several proinflammatory cytokines and chemokines in the small intestine and liver at various time points p.i. using multiplex reverse transcription (RT)-PCR. These studies demonstrated that the expression levels of TNF-α, IL-1β, MIG, eotaxin, MIP-1α, and MIP-1β gradually increased during infection, reaching a maximum at the time that infected mice were succumbing (Fig. 5). At this time,

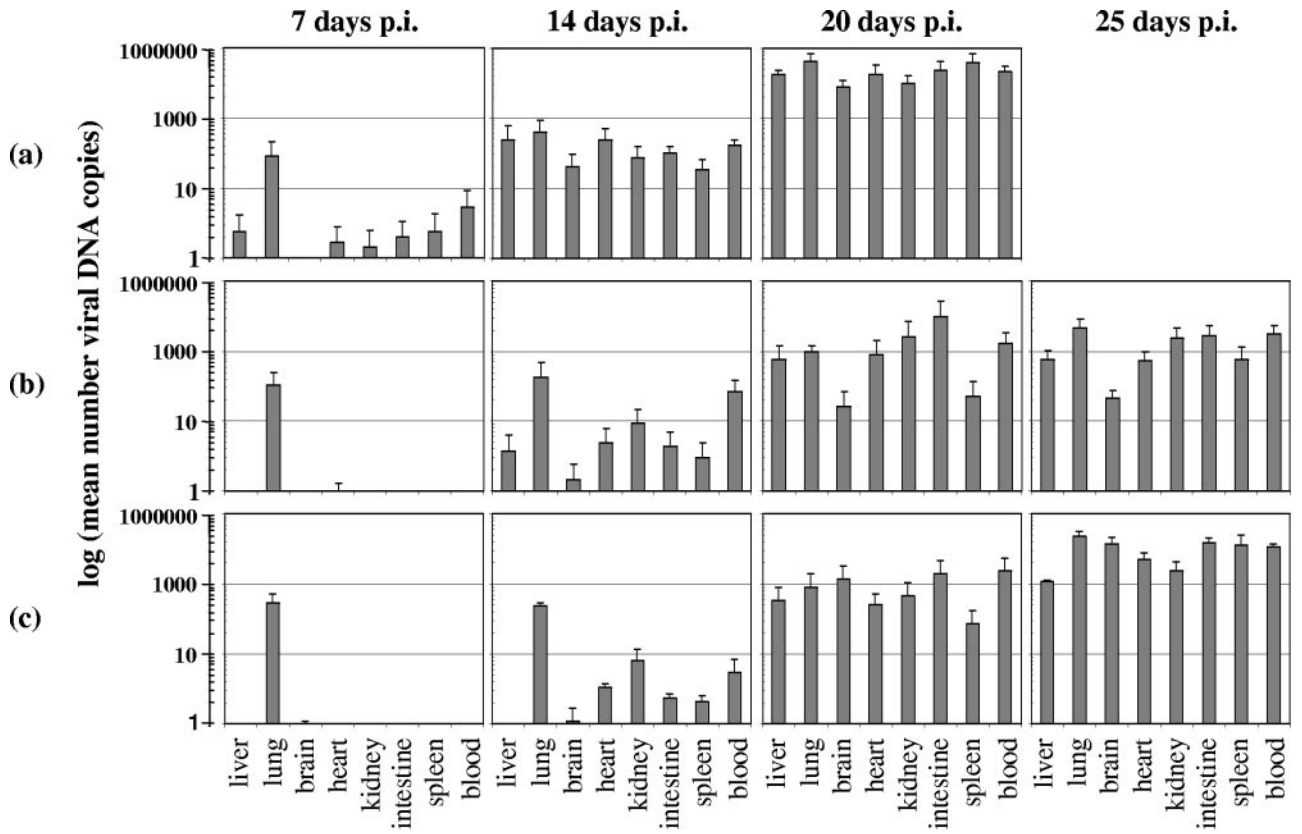

FIG. 3. Effect of antiviral therapy on viral DNA levels in infected tissues of placebo (a), cidofovir-treated (b), and S-2242-treated (c) mice at different times p.i. Data are presented as logarithmic means of the number of viral DNA copies per ng chromosomal DNA. Each bar represents the mean value ± standard deviation of the results for 4 mice.

IL-1β and ENA-78 mRNAs were clearly present in the small intestines of infected mice, while being undetectable in the intestines of noninfected mice. The mRNA levels of TNF-α, MIG, eotaxin, MIP-1α, and MIP-1β were increased about threefold compared to the levels seen in noninfected mice. In the livers of infected mice, the mRNA increase for TNF-α and MIG was comparable to what was seen in the small intestine, whereas the upregulation of IL-1β, eotaxin, MIP-1α, and MIP-1β in the liver was less pronounced. The mRNA levels of IL-6 showed no difference between infected and noninfected mice, while the mRNAs of mouse KC, MIP-2, and IFN-γ were undetectable in both infected and noninfected mice (data not shown). The induced proinflammatory cytokines and chemokines in MAV-1-infected mice, such as TNF-α, IL-1β, MIG, eotaxin, ENA-78, MIP-1α, and MIP-1β, can all be produced by monocyte/macrophage cells of the innate immune system (7, 44, 48). An augmented expression of ENA-78 in the small intestine of moribund mice may also result from damaged intestinal epithelial cells (26). In addition, all of these proinflammatory molecules (with the exception of MIP-1α and MIP-1β) can be produced by endothelial cells (23, 33, 36). Since MAV-1 replicates predominantly in endothelial cells, production of proinflammatory cytokines and chemokines by the infected endothelium appears to be a primary rather than a secondary phenomenon. The sharp disease onset in MAV-1-infected mice along with the elevated levels of proinflammatory cytokines and chemokines is reminiscent of septic shock syndrome (11).

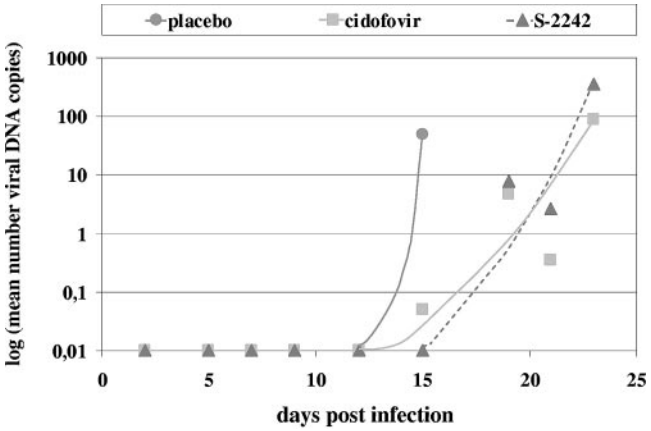

FIG. 4. MAV-1 DNA levels in urine during antiviral treatment with cidofovir or S-2242. For each time point and treatment group, DNA extracts were prepared from pooled urine samples. Data are presented as the logarithms of the number of viral DNA copies per μg creatinine.

With the aim of achieving a more-detailed insight into the organ tropism of MAV-1, SCID mice were infected with MAV-1 by intravenous infection and the subsequent pathology, inflammation, and virus distribution pattern were com-

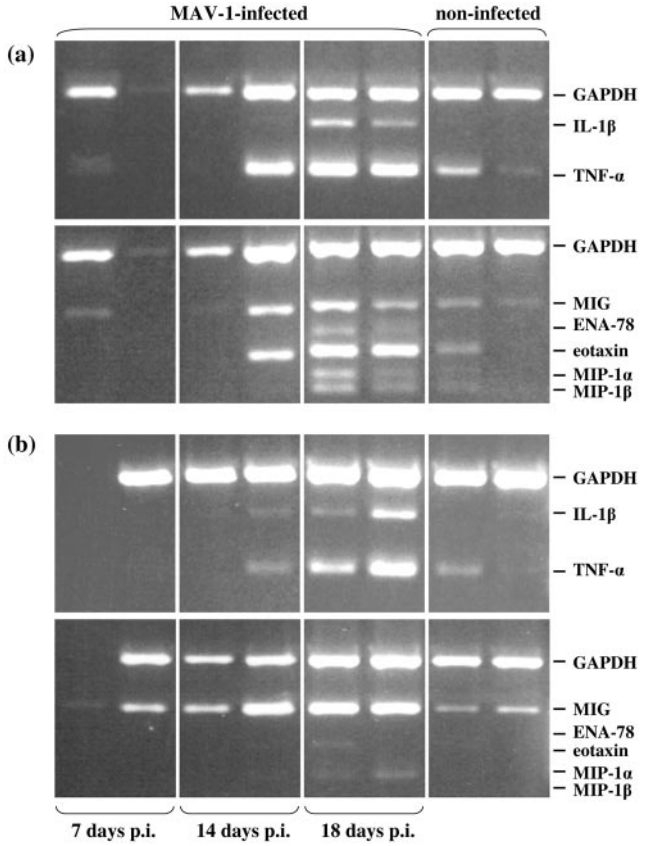

FIG. 5. mRNA expression of inflammatory cytokines and chemokines in the small intestines (a) and livers (b) of MAV-1-infected and noninfected mice. On day 7, 14, or 18 p.i., RNA extracts of the small intestine and liver were used for the evaluation of cytokine and chemokine mRNA expression, determined by multiplex RT-PCR. Noninfected mice were included as negative controls. Cytokine- and chemokine-specific bands are indicated on the right. In each box, the left and right bands represent the results for 2 mice.

pared to the observations of SCID mice infected by intranasal inoculation. Mice infected by the intravenous route succumbed significantly earlier than mice that received intranasal virus inoculation (mean day of death, 13.5 ± 0.7 and 23.5 ± 1.9 days p.i., respectively; $P = 0.0004$). However, histopathological and immunohistochemical analysis did not reveal any difference between both inoculation routes with regard to pathology, inflammation, or viral presence in affected organs. Using multiplex RT-PCR on extracts from total blood, we observed that, compared to uninfected mice, mRNA levels were slightly upregulated for the proinflammatory cytokines IL-1β and TNF-α and the chemokines MIP-1α and MIP-1β. However, the increase was approximately equal in all infected mice, irrespective of the method of virus inoculation. No transcripts could be detected for IFN-γ, MIG, ENA-78, eotaxin, KC, or MIP-2 in any of the blood samples.

In vivo evaluation of antiviral compounds. Based on the marked in vitro activity of the nucleotide analogue cidofovir against MAV-1 and Ad2, we performed two independent experiments to determine the efficacy of cidofovir in SCID mice inoculated with MAV-1 by the intranasal route. In the second experiment, we also included the nucleoside analogue S-2242, which showed in vitro activity against MAV-1 and Ad2 similar to that of cidofovir. When administered subcutaneously at 100 mg per kg for 5 consecutive days and then on alternate days, in the case of cidofovir, or by daily injection, in the case of S-2242, both antiviral drugs had a remarkably similar effect on the course of the MAV-1 infection (Fig. 1). All placebo mice, which received vehicle only, died within 22 days p.i. In contrast, cidofovir and S-2242 caused a significant and equal delay in mortality (mean day of death, 19.5 ± 1.9, 24.5 ± 1.9, and 24 ± 1.6 days p.i., for mice receiving placebo, cidofovir, and S-2242, respectively; $P \leq 0.002$ for the drug-treated groups versus placebo). Most strikingly, even while under antiviral therapy, all mice finally succumbed. At predetermined time points, mice from each treatment group were sacrificed for pathological and virologic examination. At 19 days p.i., hematoxylin and eosin staining on small intestinal tissue of placebo mice showed extensive necrosis and infiltration of neutrophils, explaining the moribund status of these mice. In contrast, no signs of pathology or inflammation were observed in the intestines of mice receiving cidofovir or S-2242 (Fig. 6). However, a few days later, when cidofovir- and S-2242-treated mice were moribund, histopathological examination revealed that the pathology and inflammation in their intestinal tissue were identical to those from the placebo mice. As described above, the inflammation in the livers of MAV-1-infected mice was found to be relatively mild. In contrast to the strong immunohistochemical staining observed on all tissues from placebo mice at 19 days p.i., staining on tissues of cidofovir- or S-2242-treated mice was negative at the same time point, except for a weak signal in the liver and spleen. Nevertheless, mice dying at ~24 days p.i., while under treatment with cidofovir or S-2242, showed the same immunohistochemical picture as moribund placebo mice (Fig. 6).

This retardation of pathological signs upon treatment with cidofovir or S-2242 was also reflected in the viral DNA content of the organs, as determined by real-time PCR (Fig. 3b and c). At the first time point (7 days p.i.), viral DNA was detected in the lungs of all infected mice (possibly reflecting residual virus after intranasal inoculation); in the other organs, viral DNA levels were low for placebo mice and undetectable for mice receiving cidofovir or S-2242. Both antiviral compounds caused a marked suppression of MAV-1 replication, albeit temporarily, since, even under antiviral therapy, the levels of viral DNA finally increased. Surprisingly, at the time cidofovir-treated mice were dying, their levels of viral DNA were, depending on the organ examined, 3- to 99-fold lower than those seen in moribund placebo mice, while this trend was less pronounced in S-2242-treated mice. Real-time PCR analysis of daily urine samples from cidofovir- or S-2242-treated mice showed that the course of viral DNA replication was delayed in time in comparison to that seen in urine samples from placebo mice (Fig. 4). At 15 days p.i., viral DNA levels were strongly increased in urine samples from placebo mice, while virtually no viral DNA was detected in urine from cidofovir- or S-2242-treated mice. In cidofovir- and S-2242-treated mice, viral DNA remained almost undetectable until the onset of clinical symptoms, and then the viral DNA concentration in urine abruptly increased, rising further until the death of the mice.

To assess drug-associated toxicity, uninfected animals were administered cidofovir or S-2242 by following the same scheme

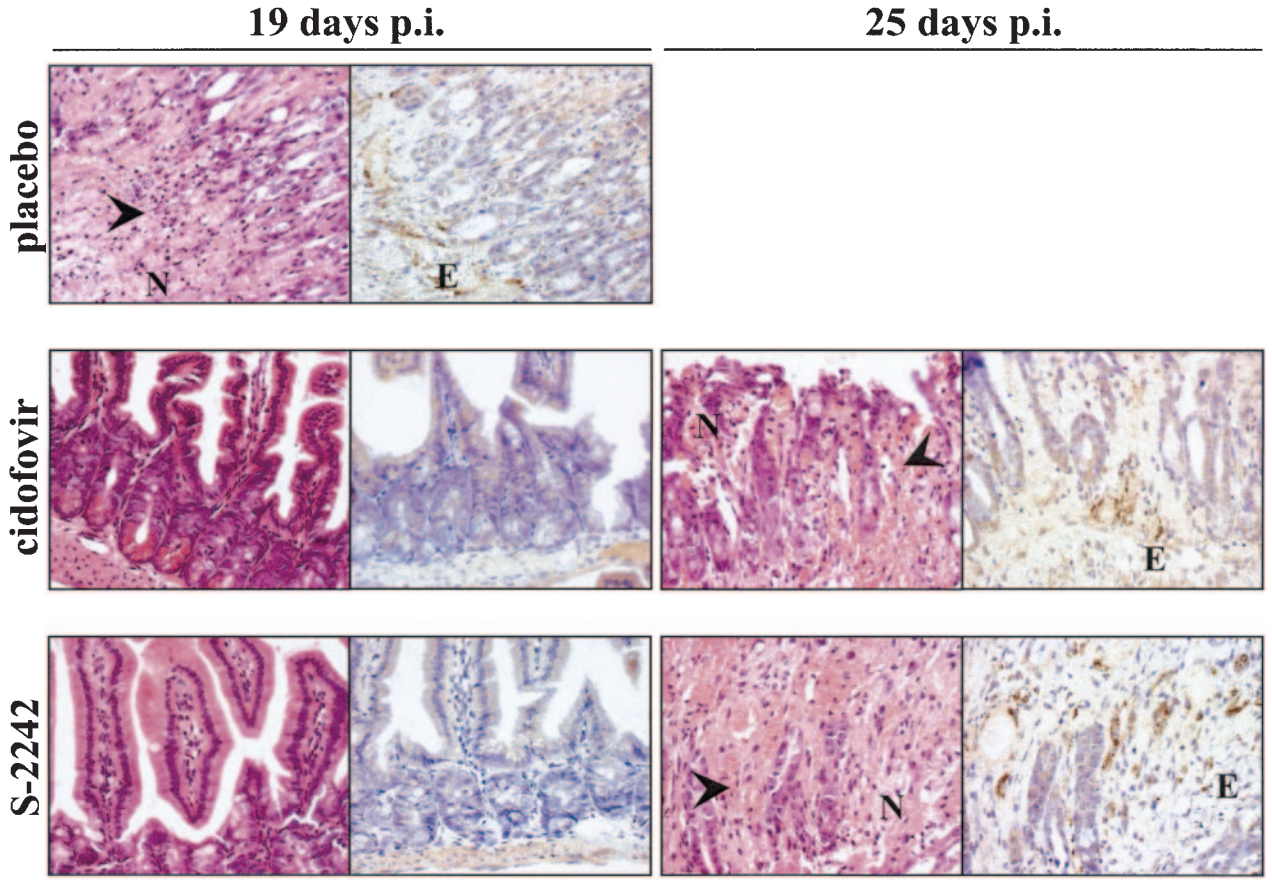

FIG. 6. Hematoxylin and eosin (left side) and immunohistochemical (right side) staining for MAV-1 E3 protein on representative sections of small intestine taken at 19 or 25 days p.i. from MAV-1-infected mice treated with placebo, cidofovir, or S-2242. Magnification, ×400. Infected cells show dark brown cytoplasmic staining for MAV-1 E3. Arrowheads indicate sites of necrosis. E, endothelial cell; N, neutrophils.

as described for the virus-infected animals, and the body weight of all mice was monitored daily. While body weight gain was normal in S-2242-treated mice (13% increase over a 24-day period), it was apparent that the dose of 100 mg cidofovir per kg represented the maximum tolerated dose. The body weight showed no increase in female cidofovir-treated noninfected mice, while male mice receiving cidofovir lost 25% of their body weight over 24 days. Upon histopathological analysis, neither pathology nor inflammation was observed in any of the examined organs of uninfected mice treated with cidofovir or S-2242.

To address the possibility that drug-resistant mutants may arise during cidofovir or S-2242 treatment, virus was isolated from the MAV-1-infected mice and tested in vitro for sensitivity to cidofovir and S-2242. At the time of severe illness, a part of the liver from mice receiving placebo, cidofovir, or S-2242 was collected, homogenized, and titrated using a standard plaque assay (54). The antiviral sensitivity of the virus present in those liver homogenates was determined in a CPE reduction assay and by real-time PCR quantification of viral DNA. For cidofovir as well as S-2242, EC_{50}s were similar for liver isolates from mice receiving either placebo, cidofovir, or S-2242, thus excluding the issue that MAV-1 may have acquired resistance to cidofovir or S-2242 in our in vivo studies.

DISCUSSION

In the present study, we have attempted to broaden our insight into the pathogenesis of the fatal disseminated disease induced by MAV-1 in SCID mice, which is characterized by hemorrhagic enteritis. Insight into the pathological, inflammatory, and viral aspects of this mouse model has assisted us in the evaluation of antiviral therapy for disseminated adenovirus infections.

As mentioned earlier, MAV-1 has a different disease outcome depending on the mouse strain. Whereas MAV-1 causes a fatal hemorrhagic encephalomyelitis in adult C57BL/6 mice, adult mice with a BALB/c background are resistant (18, 28). Yet, MAV-1 infection is lethal in adult immunocompromised BALB/c mice (38, 43). As a model for the life-threatening systemic adenovirus infections in immunocompromised patients, we infected BALB/c SCID mice intranasally with MAV-1. During a period of 17 to 19 days, the mice showed no signs of clinical illness, and afterwards, death came very rapidly. This rapid disease progress seemed to be highly reproducible. We optimized several techniques to monitor the pathology and viral aspects of MAV-1 infection. Histopathological analysis revealed that hemorrhagic enteritis was the main cause of death in our model, as described earlier for

MAV-1-infected outbred and BALB/c SCID mice (10, 28). Pirofski and colleagues reported that MAV-1 infection of SCID mice resulted in microvesicular fatty hepatocyte degeneration without significant inflammation or necrosis of the liver (43). In contrast, we did not observe this kind of liver pathology, yet liver infiltration of inflammatory cells with the formation of microabscesses was noted occasionally. However, the use of a nonpurified virus inoculum in the study of Pirofski et al. is a major difference with ours and provides an explanation for the discrepancy in the observed liver pathology. Our data are concordant with a study of Moore et al., who concluded that T cells play a key role in the induction of acute MAV-1 infection (38). This explains the absence of MAV-1-induced hepatitis in SCID mice (which lack both B and T cells) and the presence of hepatic necrosis in MAV-1-infected B-cell-deficient mice. In our studies, some mild inflammation in the liver of infected SCID mice was sporadically detected. Most likely, this inflammation does not result from a primary hepatitis but rather from migration of the inflammation from the intestinal tissue to the liver via the portal system. Using immunohistochemistry with a polyclonal antiserum directed toward an early MAV-1 protein, viral antigen was demonstrated in the endothelial cells of the intestine, liver, lung, brain, heart, kidney, and spleen tissues. This endothelial cell tropism of MAV-1 is in agreement with previous reports (10, 24). Viral antigen was also detected in hepatocytes and Kupffer cells of the liver. MAV-1 infection of hepatocytes in BALB/c SCID mice was also reported by Charles et al., but unlike us, they observed no staining of the vascular endothelium in the liver and spleen (10). In addition, unlike us and others, Charles et al. did not detect replication of MAV-1 in the brains of BALB/c SCID mice and they postulated that there may be a receptor difference between mouse strains that differ in their susceptibility to MAV-1-induced hemorrhagic encephalitis (10, 52).

Further evidence for a disseminated infection was provided by real-time PCR analysis of several organs from infected mice. At 1 week p.i., viral DNA was already present in most organs, but levels were highest in the lungs, showing that the lung is the first site of MAV-1 replication after intranasal infection. This is most likely followed by viremia and dissemination to the target organs. This fatal disseminated adenovirus infection in BALB/c SCID mice is reminiscent of the clinical situation of adenovirus infection in humans in several aspects. (i) Human adenovirus infections are mostly mild and self-limiting in healthy individuals but can cause severe or lethal illness in immunocompromised patients. (ii) In these patients, a disseminated infection is common. (iii) Enteritis, hemorrhagic cystitis, and hepatitis are common manifestations, while adenovirus encephalitis is relatively rare in humans (6, 9, 27). In retrospective and prospective studies, PCR detection of human adenovirus in blood was directly associated with disseminated adenovirus disease, which often has a fatal outcome (9, 13, 32, 47).

Since the availability of antiviral drugs for adenovirus infections remains unsatisfactory, there is an increasing need for new, effective, and safe antiadenovirus therapeutics. With this in mind, we used our MAV-1/SCID model to evaluate the nucleoside analogues cidofovir and S-2242 in the treatment of systemic adenovirus infections. In vitro, cidofovir and S-2242 showed comparable and promising activity against MAV-1 and Ad2. In vivo, cidofovir and S-2242 caused a considerable delay in MAV-1-induced disease, as demonstrated by clinical observations and histopathological, immunohistochemical, and real-time PCR analysis of dissected organs. However, cidofovir and S-2242 were not able to eradicate the virus, since all treated mice ultimately succumbed despite continued drug treatment. The acyclic nucleoside phosphonate analogue cidofovir has a long intracellular half-life, enabling an infrequent dosing scheme. Tissue distribution studies with rats demonstrated that the highest cidofovir concentrations are present in the kidneys, followed by those in the liver, lung, and intestine (40). Tissue distribution of S-2242, which is the only known N-7-substituted nucleoside analogue with activity against DNA viruses, has been poorly studied (3). Cidofovir and S-2242 have similar in vitro activities against MAV-1, and the in vitro sensitivity of MAV-1 to cidofovir and S-2242 is comparable to those of several herpesviruses. Although the doses in our in vivo studies are comparable to those used in animal studies with herpesviruses, it seems that cidofovir and S-2242 are less effective in inhibiting mortality in the MAV-1/SCID model than in the herpesvirus models (40–42). It is rather unlikely that the limited effectiveness of cidofovir and S-2242 in our MAV-1 model is due to poor disposition, since both antiviral drugs are supposed to have different pharmacokinetics and organ distribution. Apparently, the MAV-1/SCID model is a very stringent model due to the complete absence of an adaptive immune component which, under normal circumstances, is critical for viral clearance during an infection. In MAV-1-infected SCID mice, complete eradication of the virus is solely dependent on the antiviral therapy. The same holds true for the clinical situation in adenovirus-infected humans. In several retrospective studies, the failure of antiadenovirus treatment was observed in heavily immunosuppressed patients who had received a T-cell-depleted graft or suffered from severe graft-versus-host disease. The reduction of immunosuppression, combined with antiviral therapy initiated as early as possible after the adenovirus infection, remains the mainstay of therapy (1, 8, 9, 22). Alternatively, there may be a therapeutic benefit with adenovirus-specific T cells, similar to that described for Epstein-Barr virus and cytomegalovirus (46, 50). Due to extensive cross-reactivity of adenovirus-specific T cells across serotypes, this approach may be feasible (20, 51).

Finally, it is possible that the MAV-1 pathology has an important inflammatory component which is not suppressed by antiviral therapy. The inflammatory character of MAV-1 disease is demonstrated by our experiments measuring the mRNA levels of several proinflammatory cytokines and chemokines in the small intestine and liver. In MAV-1-infected mice, there was an upregulation of TNF-α, IL-1β, MIG, eotaxin, MIP-1α, and MIP-1β. In our antiviral experiments, we restricted the mRNA detection of proinflammatory cytokines and chemokines to blood leukocytes and observed little differences between infected mice whether treated or not with cidofovir or S-2242. Thus, in the MAV-1/SCID model described here, the upregulation of proinflammatory cytokines and chemokines seems to be confined to the diseased tissues (i.e., intestine and liver).

Although there is little information concerning immunologic changes in patients with adenovirus infections, a few reports describe increased levels of IL-6, IL-8, TNF-α, IL-1β, or IFN-γ

in serum in patients with severe respiratory tract infections (12, 34, 37). Recently, the hepatotoxicity of adenovirus vectors in mice was associated with the induction of TNF-α (14). A detailed study on the contribution of immunological factors in the MAV-1 pathology has now been planned.

In conclusion, the MAV-1/SCID model is a reproducible and appropriate model for the evaluation of antiviral drugs against disseminated adenovirus infections. We found that the antiviral compounds cidofovir and S-2242 can cause a significant delay in MAV-1 disease and related death but are not able to eradicate the virus. This is most likely due to the stringency of this MAV-1/SCID model, in which suppression of viral replication is not accompanied by an adequate adaptive immune response. In the clinical setting of transplant patients with severe adenovirus infections, therapeutic success will depend on the concerted action of antiviral drugs and a restored immune response, ultimately resulting in viral clearance.

ACKNOWLEDGMENTS

We thank Willy Zeegers, Wim van Dam, and Lieze Wolput for excellent technical assistance and N. Blanckaert from the Department of Laboratory Medicine, University Hospitals Leuven, for help with the creatinine determination of the urine samples.

These investigations were supported by grants from the Flemish Fonds voor Wetenschappelijk Onderzoek (FWO no. G.0267.04) and the Belgian (Flemish Community) "Geconcerteerde Onderzoeksacties" (GOA no. 2000/12). L.L. is a Research Assistant of the FWO.

REFERENCES

1. **Avivi, I., S. Chakrabarti, D. W. Milligan, H. Waldmann, G. Hale, H. Osman, K. N. Ward, C. D. Fegan, K. Yong, A. H. Goldstone, D. C. Linch, and S. Mackinnon.** 2004. Incidence and outcome of adenovirus disease in transplant recipients after reduced-intensity conditioning with alemtuzumab. Biol. Blood Marrow Transplant. **10:**186–194.
2. **Balzarini, J., R. Pauwels, M. Baba, P. Herdewijn, E. De Clercq, S. Broder, and D. G. Johns.** 1988. The in vitro and in vivo anti-retrovirus activity, and intracellular metabolism of 3′-azido-2′,3′-dideoxythymidine and 2′,3′-dideoxycytidine are highly dependent on the cell species. Biochem. Pharmacol. **37:**897–903.
3. **Besen, G., E. Chavez-de la Paz, M. Tatebayashi, M. Flores-Aguilar, P. A. Gangan, D. Munguia, C. A. Wiley, G. Jahne, I. Winkler, and M. Helsberg.** 1995. Evaluation of retinal toxicity and efficacy of the anticytomegalovirus compound 2-amino-7-[(1,3-dihydroxy-2-propoxy)methyl]purine. Antimicrob. Agents Chemother. **39:**1485–1488.
4. **Billiau, A., H. Sobis, H. Eyssen, and H. Van den Berghe.** 1973. Non-infectious intracisternal A-type particles in a sarcoma-positive, leukemia-negative mouse cell line transformed by murine sarcoma virus (MSV). Arch. Gesamte Virusforsch. **43:**345–351.
5. **Bordigoni, P., A. S. Carret, V. Venard, F. Witz, and A. Le Faou.** 2001. Treatment of adenovirus infections in patients undergoing allogeneic hematopoietic stem cell transplantation. Clin. Infect. Dis. **32:**1290–1297.
6. **Carrigan, D. R.** 1997. Adenovirus infections in immunocompromised patients. Am. J. Med. **102:**71–74.
7. **Cavaillon, J. M.** 1994. Cytokines and macrophages. Biomed. Pharmacother. **48:**445–453.
8. **Chakrabarti, S., K. E. Collingham, C. D. Fegan, and D. W. Milligan.** 1999. Fulminant adenovirus hepatitis following unrelated bone marrow transplantation: failure of intravenous ribavirin therapy. Bone Marrow Transplant. **23:**1209–1211.
9. **Chakrabarti, S., V. Mautner, H. Osman, K. E. Collingham, C. D. Fegan, P. E. Klapper, P. A. Moss, and D. W. Milligan.** 2002. Adenovirus infections following allogeneic stem cell transplantation: incidence and outcome in relation to graft manipulation, immunosuppression, and immune recovery. Blood **100:**1619–1627.
10. **Charles, P. C., J. D. Guida, C. F. Brosnan, and M. S. Horwitz.** 1998. Mouse adenovirus type-1 replication is restricted to vascular endothelium in the CNS of susceptible strains of mice. Virology **245:**216–228.
11. **Cohen, J.** 2002. The immunopathogenesis of sepsis. Nature **420:**885–891.
12. **Devergne, O., M. Peuchmaur, M. Humbert, E. Navratil, M. B. Leger-Ravet, M. C. Crevon, M. A. Petit, P. Galanaud, and D. Emilie.** 1991. In vivo expression of IL-1 beta and IL-6 genes during viral infections in human. Eur. Cytokine Netw. **2:**183–194.
13. **Echavarria, M., M. Forman, M. J. van Tol, J. M. Vossen, P. Charache, and A. C. Kroes.** 2001. Prediction of severe disseminated adenovirus infection by serum PCR. Lancet **358:**384–385.
14. **Engler, H., T. Machemer, J. Philopena, S. F. Wen, E. Quijano, M. Ramachandra, V. Tsai, and R. Ralston.** 2004. Acute hepatotoxicity of oncolytic adenoviruses in mouse models is associated with expression of wild-type E1a and induction of TNF-alpha. Virology **328:**52–61.
15. **Gavin, P. J., and B. Z. Katz.** 2002. Intravenous ribavirin treatment for severe adenovirus disease in immunocompromised children. Pediatrics **110:**e9.
16. **Ginsberg, H. S., L. L. Moldawer, P. B. Sehgal, M. Redington, P. L. Kilian, R. M. Chanock, and G. A. Prince.** 1991. A mouse model for investigating the molecular pathogenesis of adenovirus pneumonia. Proc. Natl. Acad. Sci. USA **88:**1651–1655.
17. **Gordon, Y. J., E. Romanowski, and T. Araullo-Cruz.** 1992. An ocular model of adenovirus type 5 infection in the NZ rabbit. Investig. Ophthalmol. Vis. Sci. **33:**574–580.
18. **Guida, J. D., G. Fejer, L. A. Pirofski, C. F. Brosnan, and M. S. Horwitz.** 1995. Mouse adenovirus type 1 causes a fatal hemorrhagic encephalomyelitis in adult C57BL/6 but not BALB/c mice. J. Virol. **69:**7674–7681.
19. **Hartline, C. B., K. M. Gustin, W. B. Wan, S. L. Ciesla, J. R. Beadle, K. Y. Hostetler, and E. R. Kern.** 2005. Ether lipid-ester prodrugs of acyclic nucleoside phosphonates: activity against adenovirus replication in vitro. J. Infect. Dis. **191:**396–399.
20. **Heemskerk, B., L. A. Veltrop-Duits, T. van Vreeswijk, M. M. ten Dam, S. Heidt, R. E. Toes, M. J. van Tol, and M. W. Schilham.** 2003. Extensive cross-reactivity of CD4+ adenovirus-specific T cells: implications for immunotherapy and gene therapy. J. Virol. **77:**6562–6566.
21. **Hoffman, J. A., A. J. Shah, L. A. Ross, and N. Kapoor.** 2001. Adenoviral infections and a prospective trial of cidofovir in pediatric hematopoietic stem cell transplantation. Biol. Blood Marrow Transplant. **7:**388–394.
22. **Hromas, R., C. Clark, C. Blanke, G. Tricot, K. Cornetta, A. Hedderman, and E. R. Broun.** 1994. Failure of ribavirin to clear adenovirus infections in T cell-depleted allogeneic bone marrow transplantation. Bone Marrow Transplant. **14:**663–664.
23. **Imaizumi, T., K. H. Albertine, D. L. Jicha, T. M. McIntyre, S. M. Prescott, and G. A. Zimmerman.** 1997. Human endothelial cells synthesize ENA-78: relationship to IL-8 and to signaling of PMN adhesion. Am. J. Respir. Cell Mol. Biol. **17:**181–192.
24. **Kajon, A. E., C. C. Brown, and K. R. Spindler.** 1998. Distribution of mouse adenovirus type 1 in intraperitoneally and intranasally infected adult outbred mice. J. Virol. **72:**1219–1223.
25. **Kaneko, H., S. Mori, O. Suzuki, T. Iida, S. Shigeta, M. Abe, S. Ohno, K. Aoki, and T. Suzutani.** 2004. The cotton rat model for adenovirus ocular infection: antiviral activity of cidofovir. Antivir. Res. **61:**63–66.
26. **Keates, S., A. C. Keates, E. Mizoguchi, A. Bhan, and C. P. Kelly.** 1997. Enterocytes are the primary source of the chemokine ENA-78 in normal colon and ulcerative colitis. Am. J. Physiol. **273:**G75–G82.
27. **Kojaoghlanian, T., P. Flomenberg, and M. S. Horwitz.** 2003. The impact of adenovirus infection on the immunocompromised host. Rev. Med. Virol. **13:**155–171.
28. **Kring, S. C., C. S. King, and K. R. Spindler.** 1995. Susceptibility and signs associated with mouse adenovirus type 1 infection of adult outbred Swiss mice. J. Virol. **69:**8084–8088.
29. **Lalezari, J. P., and B. D. Kuppermann.** 1997. Clinical experience with cidofovir in the treatment of cytomegalovirus retinitis. J. Acquir. Immune Defic. Syndr. Hum. Retrovirol. **14**(Suppl. 1)**:**S27–S31.
30. **Lankester, A. C., B. Heemskerk, E. C. Claas, M. W. Schilham, M. F. Beersma, R. G. Bredius, M. J. van Tol, and A. C. Kroes.** 2004. Effect of ribavirin on the plasma viral DNA load in patients with disseminating adenovirus infection. Clin. Infect. Dis. **38:**1521–1525.
31. **Legrand, F., D. Berrebi, N. Houhou, F. Freymuth, A. Faye, M. Duval, J. F. Mougenot, M. Peuchmaur, and E. Vilmer.** 2001. Early diagnosis of adenovirus infection and treatment with cidofovir after bone marrow transplantation in children. Bone Marrow Transplant. **27:**621–626.
32. **Lion, T., R. Baumgartinger, F. Watzinger, S. Matthes-Martin, M. Suda, S. Preuner, B. Futterknecht, A. Lawitschka, C. Peters, U. Potschger, and H. Gadner.** 2003. Molecular monitoring of adenovirus in peripheral blood after allogeneic bone marrow transplantation permits early diagnosis of disseminated disease. Blood **102:**1114–1120.
33. **Mancardi, S., E. Vecile, N. Dusetti, E. Calvo, G. Stanta, O. R. Burrone, and A. Dobrina.** 2003. Evidence of CXC, CC and C chemokine production by lymphatic endothelial cells. Immunology **108:**523–530.
34. **Matsubara, T., T. Inoue, N. Tashiro, K. Katayama, T. Matsuoka, and S. Furukawa.** 2000. Activation of peripheral blood CD8+ T cells in adenovirus infection. Pediatr. Infect. Dis. J. **19:**766–768.
35. **Meissner, J. D., G. N. Hirsch, E. A. LaRue, R. A. Fulcher, and K. R. Spindler.** 1997. Completion of the DNA sequence of mouse adenovirus type 1: sequence of E2B, L1, and L2 (18–51 map units). Virus Res. **51:**53–64.
36. **Menzies-Gow, A., S. Ying, S. Phipps, and A. B. Kay.** 2004. Interactions between eotaxin, histamine and mast cells in early microvascular events associated with eosinophil recruitment to the site of allergic skin reactions in humans. Clin. Exp. Allergy **34:**1276–1282.
37. **Mistchenko, A. S., R. A. Diez, A. L. Mariani, J. Robaldo, A. F. Maffey, G.**

Bayley-Bustamante, and S. Grinstein. 1994. Cytokines in adenoviral disease in children: association of interleukin-6, interleukin-8, and tumor necrosis factor alpha levels with clinical outcome. J. Pediatr. **124:**714–720.
38. **Moore, M. L., E. L. McKissic, C. C. Brown, J. E. Wilkinson, and K. R. Spindler.** 2004. Fatal disseminated mouse adenovirus type 1 infection in mice lacking B cells or Bruton's tyrosine kinase. J. Virol. **78:**5584–5590.
39. **Naesens, L., L. Lenaerts, G. Andrei, R. Snoeck, D. Van Beers, A. Holy, J. Balzarini, and E. De Clercq.** 2005. Antiadenovirus activities of several classes of nucleoside and nucleotide analogues. Antimicrob. Agents Chemother. **49:**1010–1016.
40. **Naesens, L., R. Snoeck, G. Andrei, J. Balzarini, J. Neyts, and E. De Clercq.** 1997. HPMPC (cidofovir), PMEA (adefovir) and related acyclic nucleoside phosphonate analogues: a review of their pharmacology and clinical potential in the treatment of viral infections. Antivir. Chem. Chemother. **8:**1–23.
41. **Neyts, J., G. Andrei, R. Snoeck, G. Jahne, I. Winkler, M. Helsberg, J. Balzarini, and E. De Clercq.** 1994. The N-7-substituted acyclic nucleoside analog 2-amino-7-[(1,3-dihydroxy-2-propoxy)methyl]purine is a potent and selective inhibitor of herpesvirus replication. Antimicrob. Agents Chemother. **38:**2710–2716.
42. **Neyts, J., G. Jahne, G. Andrei, R. Snoeck, I. Winkler, and E. De Clercq.** 1995. In vivo antiherpesvirus activity of N-7-substituted acyclic nucleoside analog 2-amino-7-[(1,3-dihydroxy-2-propoxy)methyl]purine. Antimicrob. Agents Chemother. **39:**56–60.
43. **Pirofski, L., M. S. Horwitz, M. D. Scharff, and S. M. Factor.** 1991. Murine adenovirus infection of SCID mice induces hepatic lesions that resemble human Reye syndrome. Proc. Natl. Acad. Sci. USA **88:**4358–4362.
44. **Ponath, P. D., S. Qin, D. J. Ringler, I. Clark-Lewis, J. Wang, N. Kassam, H. Smith, X. Shi, J. A. Gonzalo, W. Newman, J. C. Gutierrez-Ramos, and C. R. Mackay.** 1996. Cloning of the human eosinophil chemoattractant, eotaxin. Expression, receptor binding, and functional properties suggest a mechanism for the selective recruitment of eosinophils. J. Clin. Investig. **97:**604–612.
45. **Prince, G. A., D. D. Porter, A. B. Jenson, R. L. Horswood, R. M. Chanock, and H. S. Ginsberg.** 1993. Pathogenesis of adenovirus type 5 pneumonia in cotton rats (Sigmodon hispidus). J. Virol. **67:**101–111.
46. **Regn, S., S. Raffegerst, X. Chen, D. Schendel, H. J. Kolb, and M. Roskrow.** 2001. Ex vivo generation of cytotoxic T lymphocytes specific for one or two distinct viruses for the prophylaxis of patients receiving an allogeneic bone marrow transplant. Bone Marrow Transplant. **27:**53–64.
47. **Schilham, M. W., E. C. Claas, W. van Zaane, B. Heemskerk, J. M. Vossen, A. C. Lankester, R. E. Toes, M. Echavarria, A. C. Kroes, and M. J. van Tol.** 2002. High levels of adenovirus DNA in serum correlate with fatal outcome of adenovirus infection in children after allogeneic stem-cell transplantation. Clin. Infect. Dis. **35:**526–532.
48. **Schnyder-Candrian, S., and A. Walz.** 1997. Neutrophil-activating protein ENA-78 and IL-8 exhibit different patterns of expression in lipopolysaccharide- and cytokine-stimulated human monocytes. J. Immunol. **158:**3888–3894.
49. **Smee, D. F., K. W. Bailey, and R. W. Sidwell.** 2002. Treatment of lethal cowpox virus respiratory infections in mice with 2-amino-7-[(1,3-dihydroxy-2-propoxy)methyl]purine and its orally active diacetate ester prodrug. Antiviral Res. **54:**113–120.
50. **Smith, C. A., L. S. Woodruff, G. R. Kitchingman, and C. M. Rooney.** 1996. Adenovirus-pulsed dendritic cells stimulate human virus-specific T-cell responses in vitro. J. Virol. **70:**6733–6740.
51. **Smith, C. A., L. S. Woodruff, C. Rooney, and G. R. Kitchingman.** 1998. Extensive cross-reactivity of adenovirus-specific cytotoxic T cells. Hum. Gene Ther. **9:**1419–1427.
52. **Spindler, K. R., L. Fang, M. L. Moore, G. N. Hirsch, C. C. Brown, and A. Kajon.** 2001. SJL/J mice are highly susceptible to infection by mouse adenovirus type 1. J. Virol. **75:**12039–12046.
53. **Tiensiwakul, P., and N. Khoobyarian.** 1983. Adenovirus fiber protein produces synthesis of interferon in mouse spleen and macrophage cultures. Intervirology **20:**52–55.
54. **Tollefson, A., T. Hermiston, and W. Wold.** 2005. Preparation and titration of CsCl-banded adenovirus stock, p. 1–9. *In* W. S. M Wold (ed.), Adenovirus methods and protocols. Humana Press, Totowa, N.J.
55. **Trousdale, M. D., P. L. Goldschmidt, and R. Nobrega.** 1994. Activity of ganciclovir against human adenovirus type-5 infection in cell culture and cotton rat eyes. Cornea **13:**435–439.
56. **Walls, T., A. G. Shankar, and D. Shingadia.** 2003. Adenovirus: an increasingly important pathogen in paediatric bone marrow transplant patients. Lancet Infect. Dis. **3:**79–86.